PAPER

Synthesis of site-heterologous haptens for high-affinity anti-pyraclostrobin antibody generation†

Josep V. Mercader,[a] Consuelo Agulló,[b] Antonio Abad-Somovilla*[b] and Antonio Abad-Fuentes*[a]

The design and synthesis of functional chemical derivatives of small organic molecules is usually a key step for the intricate production of a variety of bioconjugates. In this respect, the derivatization site at which the spacer arm is introduced in immunizing conjugates constitutes a highly critical parameter for the generation of high-affinity and selective antibodies. However, due to the usual complexity of the required synthetic procedures, the appropriate comparison of alternative tethering positions has often been neglected. In the present study, meticulous strategies were followed to prepare synthetic derivatives of pyraclostrobin with the same linkers located at diverse rationally-chosen sites. Activity appraisal of antibodies and bioconjugates was carried out by bidimensional competitive direct and indirect immunoassays, and a superior performance of two of the three synthesized haptens was found. Finally, a detailed analysis of the conformations of the target molecule and the synthesized haptens in aqueous solution was done using computer assisted molecular modeling techniques. This study suggested that the lower titers and affinities of one set of antibodies are most probably due to conformational effects of the spacer arm in the immunizing bioconjugate.

Introduction

The production of high-affinity and selective binders to small organic molecules is a biotechnological research field of huge importance for such diverse disciplines as drug discovery, clinical diagnostics, food safety, and environmental monitoring. Antibodies are the paradigm of binding proteins due to their exquisite molecular recognition ability. Long ago, Nobel-prize winner Karl Landsteiner was the first to discover that low molecular weight compounds become immunogenic only after association with a carrier protein, coining the term hapten for these substances.[1] Because small organic molecules usually lack ready-to-activate chemical groups for protein conjugation, the generation of high-quality antibodies exhibiting the desired ligand-binding features strongly relies on the synthesis of suitable functional derivatives of the target analyte. Such synthetic derivatives should closely mimic the target ligand, maximizing the steric, hydrophobic, and electronic similarity to the parent molecule. Most commonly, synthetic haptens incorporate a spacer arm to better display the molecule

thus facilitating its recognition by the receptor despite the fact that direct coupling of the analyte to the carrier protein, when possible, has occasionally been employed.[2] Although the physico-chemical characteristics of the analyte determine the optimum properties of the spacer arm for hapten conjugation, linear aliphatic bridges are known to cause negligible interferences over the production of antibodies if an optimum length of two to six carbon atoms is maintained.[3] Nevertheless, a critical parameter for the production of antibodies is, most noteworthy, the derivatization site; that is, the position at which the spacer arm is attached to the molecule. The linker position will mold the final conformation of the conjugate and therefore it will settle the specific moieties that will be accessible for binding. Even if these general considerations are simple and qualitative, they have generally been extremely useful—in combination with rational and judicious chemical examination of the target molecule by qualified chemists—for the synthesis of appropriate haptens and bioconjugates applied to the production of antibodies with the desired binding properties. Lately, molecular modeling techniques are being increasingly used as complementary tools to assist researchers in, for instance, the prediction of the best hapten structures for immunoconjugate preparation or the interpretation of experimental results regarding affinity or selectivity of receptors.[4]

Strobilurins are a new class of synthetic biocides displaying outstanding properties and a new mode of action, so the introduction of the first strobilurin fungicides in 1996 meant a significant contribution to the fight against fungal diseases.[5] As part of an ongoing project aimed at obtaining high-affinity antibodies and developing immunochemical methods to selectively detect the

[a]*Department of Organic Chemistry, Universitat de València, Doctor Moliner 50, 46100, Burjassot, València, Spain. E-mail: antonio.abad@uv.es; Fax: +34-963544328; Tel: +34-963544509*

[b]*Department of Biotechnology, IATA-CSIC, Agustí Escardino 7, 46980, Paterna, València, Spain. E-mail: aabad@iata.csic.es; Fax: +34-963636301; Tel: +34-963636301*

† Electronic supplementary information (ESI) available. Full characterization data of all the intermediate compounds in the synthesis of haptens PYa6 and PYs5 are given as well as complementary data about conformational studies and copies of ^{1}H NMR and MS spectra. See DOI: 10.1039/c0ob00686f

most relevant chemicals of the strobilurin family of pesticides, we chose pyraclostrobin (PY) as a model analyte to ascertain the influence of the spacer arm attachment site on the affinity of the derived antibodies. PY is considered as a second generation strobilurin fungicide, and it is composed of a methoxycarbamate toxophore moiety, an aryl bridge, and a characteristic two-ring system (Fig. 1). In this article, we describe the synthesis of PY derivatives with the spacer arm located at different sites of the molecule. To rigorously compare the suitability of these synthetic haptens for inducing the formation of high-affinity antibodies, a homogenous linker of comparable length and composition was used for coupling to the same carrier protein. Very few examples have been found in the literature in which the same spacer arm was used to prepare several functionalized haptens through different derivatization sites in order to find the optimum orientation of the molecule.[6] Antisera, representing the unbiased whole-response of the animal immune system, were chosen as the source of antibodies. The affinity and selectivity of the generated reagents were evaluated by competitive enzyme-linked immunosorbent assay (cELISA) using the conjugate-coated indirect and the antibody-coated direct formats. Finally, our results were assessed with computer-generated molecular models of the target molecule and the synthesized haptens.
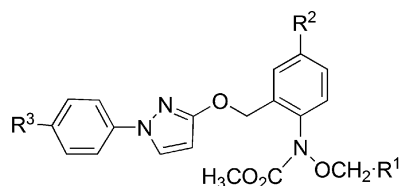
PY: R^1 = CH$_3$, R^2 = H, R^3 = Cl
Hapten PYo5: R^1 = (CH$_2$)$_3$CO$_2$H, R^2 = H, R^3 = Cl
Hapten PYa6: R^1 = CH$_3$, R^2 = (CH$_2$)$_5$CO$_2$H, R^3 = Cl
Hapten PYs5: R^1 = CH$_3$, R^2 = H, R^3 = S(CH$_2$)$_4$CO$_2$H

Fig. 1 *Structure of PY and the three synthetic haptens.*

Results and discussion

Chemistry

After a rational examination of the planar structure of PY (Fig. 1), three key positions for the introduction of the spacer arm and analyte functionalization became readily apparent: the methoxycarbamate toxophore moiety, the arylic bridge, and the chlorophenyl moiety. Accordingly, three PY analogues, namely, PYo5, PYa6, and PYs5 (Fig. 1), were proposed as haptens for the production of high-affinity antibodies. All three structures maintained the complete hydrocarbon skeleton and the most characteristic functional groups of the analyte, incorporating the hydrocarbon spacer arm at positions where minimum modifications of steric and electronic properties of the molecule were expected. Moreover, the length and composition of the spacer arms were nearly identical in all three haptens. The synthesis of haptens PYa6 and PYs5 is herein reported for the first time, whereas the preparation of hapten PYo5 was previously described by our group in a study dealing with the influence of the spacer arm length on antibody production.[7] In hapten PYa6, the spacer arm is directly attached to the aryl ring that contains the methoxycarbamate group through a single carbon-carbon bond, while in hapten PYs5 the hydrocarbon spacer chain is bonded to the other (opposite) aryl group through a sulfur bridge that replaced the chlorine atom of PY. A preliminary examination of the synthetic routes required for the preparation of haptens PYa6 and PYs5 evidenced that rather laborious and multi-step schemes would be required to prepare these analogues. Initial attempts to introduce the spacer arm at the required positions directly on PY failed, so haptens had to be finally prepared by total synthesis starting from ready available materials. We used an adaptation of the strategy previously reported for the preparation of PY[8] and related compounds,[9] which involved, for such cases, the alkylation of a 1-aryl-1H-pyrazol-3-ol with a methyl 2-(bromomethyl)-phenyl(methoxy)carbamate as the key synthetic step for the elaboration of the characteristic PY framework.

The synthesis of hapten PYa6 (**11**) began with the iodination reaction of methyl methoxy(*o*-tolyl)carbamate (**1**) using iodine and silver sulfate in AcOH (Scheme 1). This reaction is highly efficient
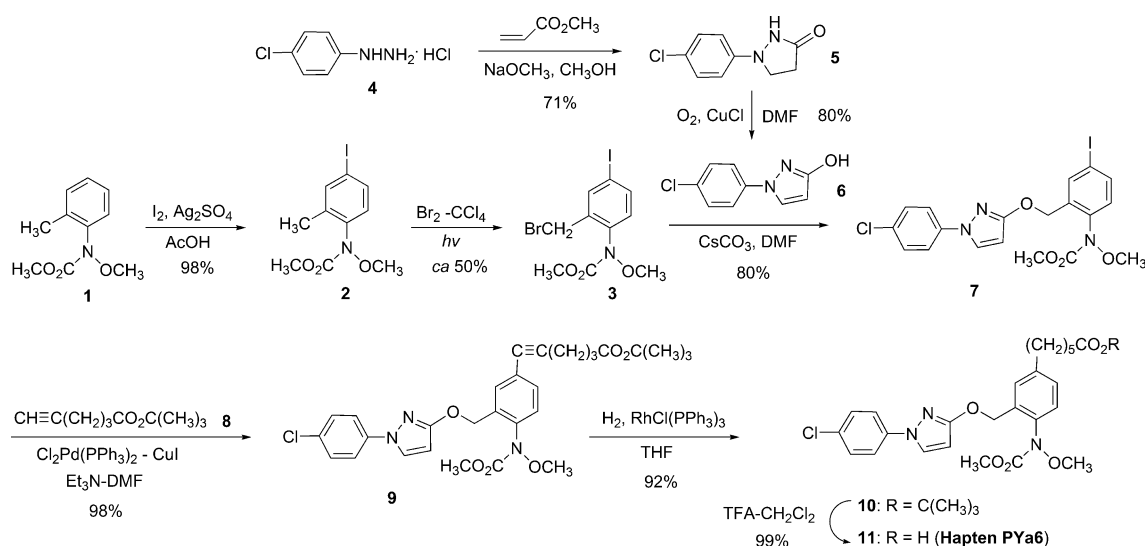
Scheme 1 Synthesis of hapten PYa6.

and regioselective, affording exclusively the 4-iodo compound **2**. Radical benzylic bromination of **2** with *N*-bromosuccinimide and azobisisobutyronitrile as the initiator under standard thermal conditions afforded a very low yield of the desired benzylic bromide, a result that contrasted with that obtained in the bromination reaction of the non iodinated analogue (see below). However, an acceptable yield of benzyl bromide **3** was obtained when the free radical bromination of iodide **2** was undertaken with bromine under radiation-induced conditions at room temperature. Under these conditions, the reaction afforded a mixture of bromide **3** and unreacted starting material, together with minor amounts of the corresponding benzylic dibrominated derivative, which could not be separated by conventional chromatographic methods, so it was used as such in the following step. Thus, the expected benzyl ether **7** was obtained in excellent yield from the reaction of this mixture with 1-(4-chlorophenyl)-1H-pyrazol-3-ol (**6**), readily prepared according to a literature procedure[10] by reaction of (4-chlorophenyl)hydrazine hydrochloride (**4**) with methyl acrylate and oxidation of the resulting pyrazolidinone **5** with oxygen and catalytic CuCl in about 57% overall yield. Once the tricyclic ring system present in PY had been prepared, the synthesis of hapten PYa6 was completed *via* substitution of the iodine atom in **7** by the C6 hydrocarbon chain using palladium catalyzed coupling methodology. Thus, Sonogashira cross-coupling of iodide **7** with alkyne *tert*-butyl ester **8** under standard conditions afforded the acetylenic compound **9**, which was hydrogenated using Wilkinson's catalyst to give compound **10** in 90% overall yield for the two steps. The synthesis of hapten PYa6 was completed by hydrolysis of the *tert*-butyl ester group of **10**, which took place in nearly quantitative yield by treatment with trifluoroacetic acid at 0 °C.

The synthesis of hapten PYs5 (**20**) began with the preparation of 1-(4-iodophenyl)-1H-pyrazol-3-ol (**14**) (Scheme 2), which was obtained from (4-iodophenyl)hydrazine (**12**) *via* a two step process involving condensation with *tert*-butyl acrylate catalyzed by potassium *tert*-butoxide and subsequent oxidation of the obtained dihydropyrazolone **13** with air catalyzed by CuCl. The pyrazolol **14** was obtained with an overall yield of about 60%. Replacement of the iodine atom in **14** by the alkyl

Table 1 Molar ratios of the different bioconjugates[a]

Hapten	BSA		OVA	HRP
	Abs.[b]	MALDI[c]	Abs.	Abs.
PYo5	19	12	5	4
PYa6	25	15	8	6
PYs5	17	17	6	3

[a] Hapten densities were calculated as moles of hapten per mole of protein.
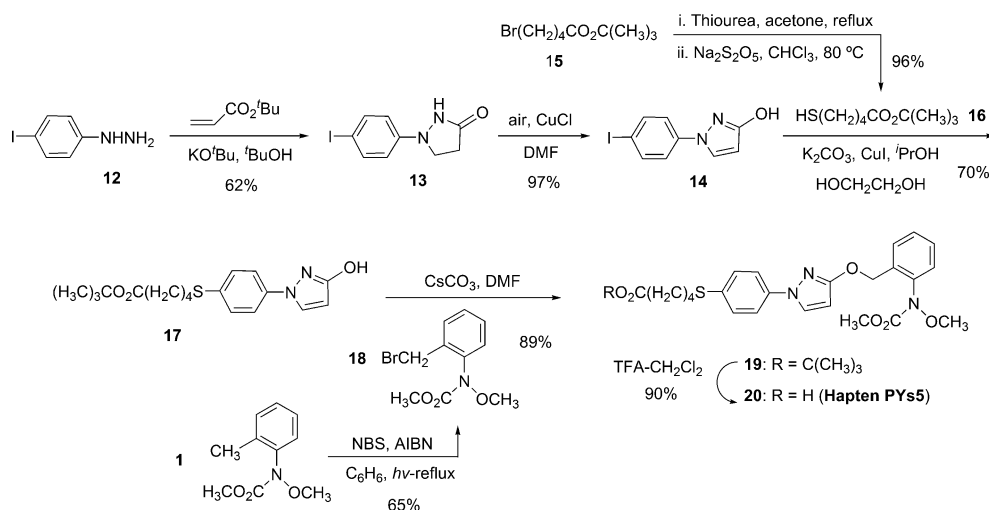[b] Hapten densities retrieved by differential absorbance measurements.
[c] Hapten densities calculated by MALDI-TOF-MS.

sulfide chain was efficiently carried out by Cu-catalyzed cross-coupling reaction of the aryl iodide with the thiol **16**, which was in turn prepared from *tert*-butyl 5-bromopentanoate (**15**) and thiourea in very high yield *via* formation of the thiouronium salt followed by cleavage with sodium pyrosulfite.[11] The synthesis of the whole framework of hapten PYs5 was completed by alkylation of the pyrazolol moiety of **14** with the known methyl 2-(bromomethyl)phenyl(methoxy)carbamate (**18**) in a similar way to that described above for the other hapten. Under these conditions, the alkylation reaction afforded the *tert*-butyl ester **19** in an excellent 89% yield. Finally, acid hydrolysis of the *tert*-butyl ester group of **19** by trifluoroacetic acid treatment gave the desired hapten PYs5 (**20**) with also an excellent yield.

Bioconjugates and antibodies

The hapten density of the immunogenic conjugates is a fundamental parameter that determines the titer and the affinity of the generated antibodies. Hapten's carboxyl groups were activated for coupling to the ε-amine residues of the carrier proteins by standard procedures (see experimental part). The hapten-to-protein molar ratios (MR) of the three bioconjugates to bovine serum albumin (BSA) were determined by differential absorbance measurements and MALDI-TOF-MS. Similar values were retrieved by both analytical methods (Table 1) as also observed by other authors,[12] except for the MR of BSA–PYa6 when calculated by differential absorption, which seemed to be overestimated. Anyhow,

Scheme 2 Synthesis of hapten PYs5.

This journal is © The Royal Society of Chemistry 2011

Org. Biomol. Chem., 2011, **9**, 1443–1453 | 1445

Table 2 Assay parameters achieved with homologous conjugates in the two cELISA formats

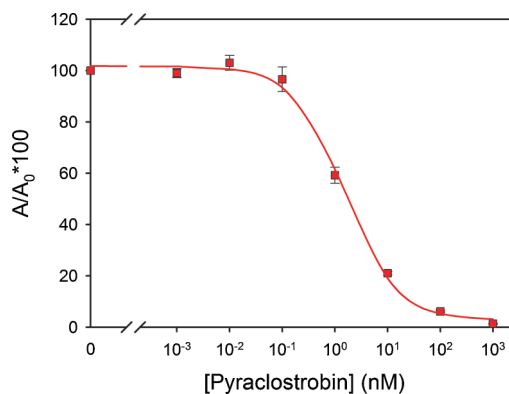| Antiserum	Indirect cELISA[a]			Direct cELISA[b]		
	Antiserum dilution ($\times 10^3$)	A_{max}	IC_{50}	[Tracer] (ng mL^{-1})	A_{max}	IC_{50}
rPYo5#1	30	1.40 ± 0.29	4.9 ± 2.0	300	0.94 ± 0.09	10.2 ± 0.9
rPYo5#2	30	1.24 ± 0.14	6.8 ± 1.8	100	0.93 ± 0.26	8.4 ± 2.6
rPYa6#1	3	0.90 ± 0.25	14.4 ± 4.5	300	0.87 ± 0.01	> 100
rPYa6#2	10^c	1.19 ± 0.01	43.0 ± 5.9	300	0.46 ± 0.07^d	> 100
rPYs5#1	10	0.92 ± 0.33	5.0 ± 1.0	30	1.38 ± 0.18	6.9 ± 1.1
rPYs5#2	10	0.85 ± 0.09	1.7 ± 0.8	10	0.86 ± 0.12	1.5 ± 0.3

[a] Coating with homologous conjugate at 100 ng mL^{-1}. [b] Antibody dilution was 1/3000. [c] Assay obtained with 1.0 µg mL^{-1} homologous conjugate. [d] A_{max} above 0.5 could not be reached.

equivalent MRs for the three immunogens were found as required for a proper comparison of the immune response. The observed MRs of our BSA conjugates were in the same range as the optimum MRs for immunogenic conjugates determined by Boro *et al.*[13] using the same carrier protein. For assay conjugates, carrier proteins different to the immunogen are demanded, so ovalbumin (OVA) and horseradish peroxidase (HRP) were employed. Considering the calculated MRs of these conjugates, it could also be seen that both of the PYa6 assay conjugates were slightly higher than those of the other haptens, as it happened with the BSA–PYa6 conjugate. Unfortunately, the MRs of OVA conjugates could not be determined by MALDI-TOF-MS, and the same mass spectra were obtained for the unconjugated and the conjugated HRP samples, probably due to the low density of hapten molecules in the conjugates. In any case, all assay (HRP and OVA) conjugates behaved correctly in the cELISA at usual concentrations, demonstrating that they carried sufficient hapten molecules for adequate assay performance.

Six rabbits were immunized and blood samples were collected after the third immunization. Titers of the two BSA–PYa6 immunized animals were approximately 10^4, whereas those of animals immunized with BSA–PYs5 and BSA–PYo5 were around 10 and 50 times higher, respectively. The titers did not improve after the fourth immunization, and consequently the animals were exsanguinated. Finally, two antisera were generated from each immunogen: antisera rPYa6#1 and #2 from immunogen BSA–PYa6, antisera rPYo5#1 and #2 from immunogen BSA–PYo5, and antisera rPYs5#1 and #2 from immunogen BSA–PYs5.

The influence of the derivatization site of assay conjugates was evaluated for the two most common cELISA formats. Depending on the ELISA format, OVA–hapten conjugates were used as passive immobilized competitive reagent for indirect assays whereas HRP–hapten conjugates were employed as enzyme tracer conjugates in direct assays. The binding properties of the generated polyclonal antibodies were initially evaluated as the IC_{50} value of the inhibition curve that was retrieved in homologous competitive assays with PY as free analyte (Table 2). Standard curves were run using an array of concentrations of the antibody and the assay conjugate, so that a family of inhibition curves was generated; one curve for each combination of immunoreagents. This approach enabled a simultaneous, and therefore comparable, determination of the IC_{50} values under different experimental conditions, so information about antibody affinity was rapidly acquired without a previous titration assay. We found that, in the conjugate-coated indirect format, the antisera generally performed

better (lower IC_{50} values) when OVA–hapten conjugates were employed at 0.1 µg mL^{-1} (Table 2). Under optimum conditions for each combination of immunoreagents, antibodies derived from haptens PYo5 and PYs5 recognized PY with a similar affinity, with antiserum rPYs5#2 displaying the lowest IC_{50} value (1.7 nM). On the contrary, antisera from hapten PYa6 showed lower affinity. These divergent results were even more evident in the antibody-coated direct format, in which antibodies from hapten PYa6 clearly did not perform as advantageously as the antibodies derived from the two other haptens. Fig. 2 shows the standard curve for the optimized assay in the antibody-coated direct cELISA format resulting from the combination of antiserum rPYs5#2 with its homologous tracer HRP–PYs5. This assay afforded a theoretical limit of detection of 0.13 nM (50 ng L^{-1}).

Fig. 2 *Standard curve for the optimized direct cELISA using antiserum rPYs5#2 and the homologous tracer.* The A_{max} value was 0.84. Values are the mean of three independent experiments.

The antibody apparent affinity that results from the calculated IC_{50} values may be influenced by the hapten conjugate that is used for solid phase coating in indirect assays or that is coupled to the enzyme in direct assays. Therefore, cELISAs were also undertaken with heterologous conjugates for each antiserum (Table 3). Both, PYs5-type antisera and PYo5-type antisera recognized the coating OVA–PYa6 conjugate. However, very modest improvements of the IC_{50} values, if any, were observed with these heterologous assays as compared with the corresponding homologous combinations. On the contrary, PYa6-type antisera did increase their apparent affinity to PY with heterologous OVA conjugates. As expected, the antibody-coated direct format was much more demanding about using heterologous haptens because no binding (or not enough

Table 3 Assay parameters achieved with heterologous conjugates in the two cELISA formats[a]

| Antiserum | Indirect cELISA[b] | | | | Direct cELISA[c] | | | |
	OVA conjugate	Antiserum dilution ($\times 10^3$)	A_{max}	IC_{50} (nM)	HRP conjugate	[Tracer] (ng mL^{-1})	A_{max}	IC_{50} (nM)
rPYo5#1	PYa6	30	1.23 ± 0.22	2.4 ± 0.3	PYa6	300	1.01 ± 0.10	6.3 ± 0.5
rPYo5#2	PYa6	10	1.57 ± 0.14	6.2 ± 1.4	PYa6	300	0.91 ± 0.22	22.2 ± 6.1
rPYa6#1	PYo5[d]	3	1.01 ± 0.32	7.5 ± 4.0				
rPYa6#2	PYo5	30	0.95 ± 0.09	15.4 ± 1.9				
rPYs5#1	PYa6	3	1.28 ± 0.32	4.2 ± 0.9				
rPYs5#2								

[a] Only results of those immunoreagent combinations that afforded A_{max} values over 0.5 are given. [b] Coating conjugate was at 1.0 µg mL^{-1}. [c] Antibody dilution was 1/3000. [d] Coating conjugate concentration was 0.1 µg mL^{-1}.

binding) to the tracer conjugate was observed in most cases. As a matter of fact, heterologous direct assays could only be developed with PYo5-derived antibodies in combination with the enzyme tracer HRP–PYa6 (Table 3). Interestingly, antiserum rPYs5#2, displaying the highest affinity to PY in the homologous assays, was the only antibody unable to recognize any heterologous haptens. Overall, the same conclusion was deduced from homologous and heterologous assays; that is, PYo5 and PYs5 haptens performed better as immunogens than hapten PYa6.

For selectivity studies, competitive assays were run in the conjugate-coated indirect format with all of the antibodies at the selected immunoreagent concentrations to give A_{max} values between 1.0 and 1.5 and using PY and other analytes as competitors. Homologous conjugates were used in each case at 0.1 µg mL^{-1}, except for antiserum rPYa6#2, for which the OVA–PYa6 conjugate was used at 1.0 µg mL^{-1}. Remarkably, no member of the strobilurin family other than PY was recognized by any of the antisera, disregarding the derivatization site of the immunogen. All of the strobilurin fungicides (azoxystrobin, picoxystrobin, kresoxim-methyl, trifloxystrobin, dimoxystrobin, fluoxastrobin, and orysastrobin) were assayed up to 1 µM. The selectivity of the six antisera towards other fungicides like boscalid, famoxadone, fenamidone, or cyazofamid, which are commonly formulated together with PY, was also investigated. Again, none of the antisera bound any of these compounds.
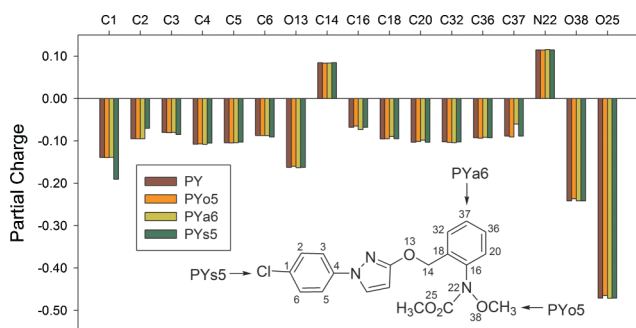
Computational analysis

PY is a medium-sized hapten with a very high degree of conformational flexibility due to the large number of bonds that display free rotation (see Table 1SI in the ESI†). As a previous step to study the molecular properties of the functionalized haptens, the lowest-energy conformers of PY in water were determined using computer assisted techniques. This molecular search resulted in a large amount of conformers (see Figure 1SI†), which were processed and analyzed as described in the experimental part (see that section for determination of minimum-energy conformations). Fig. 3 depicts the optimized geometry (PM3-H$_2$O) of the conformer that displayed the lowest energy value (refer to Figure 2SI† for the geometries of the other minimum-energy conformers, their classification and selection). Interestingly, the PY molecule, like the natural strobilurin A and several of its analogues,[14] does not adopt an extended geometry in solution. All minimum-energy conformations were characterized by two planar moieties—one plane was formed by the chlorophenyl and pyrazolyloxy moieties
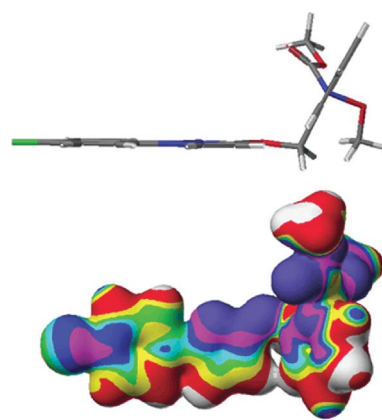
Fig. 3 *Two views of the lowest energy conformer found for PY observed from two different points of view.* In the upper structure, the elements are represented in the following manner: carbon, grey; oxygen, red; nitrogen, blue; and chlorine, green. The lower structure represents the electron density surface colored by electrostatic potential of a different view of the most stable conformation of PY. The energy values [in atomic units (au)] at each color interface are: white–red, +0.09 au; red–yellow, +0.02 au; yellow–green, +0.01 au; green–light blue, 0.00 au; light blue–dark blue, −0.01 au; dark blue–pink, −0.03 au; pink–violet, −0.06 au; where 1 au = 627.503 kcal mol^{-1}.

and the other plane was formed by the *ortho*-substituted benzene ring—with an angle between them varying from 100° to 120°. A more accurate representation of the true shape of PY is given by the electron density isosurface showed in the bottom of Fig. 3 which also reflects the electrostatic potential at every point on the surface. Electronic distribution and geometry are objective criteria to assist hapten design and interpret antibody behavior. Our experimental data clearly evidenced the advantage of haptens PYo5 and PYs5 over PYa6 with regard to the production of anti-PY antibodies (Tables 2 and 3). Sanvicens *et al.*[15] found that the best antibody for trichloroanisol was obtained with an immunizing hapten in which the spacer arm had been introduced by substitution of a C–Cl bond by a C–C linkage, which made the aromatic carbon atom much more positive. In contrast, the electronic distribution played a major role in the production of antibodies against trichlorophenol.[6b] To gain some insights into the molecular reasons underlying our results, the electronic properties of the three haptens were simulated by attaching the linkers to the appropriate position of the lowest-energy PY conformer. As depicted in Fig. 4, the introduction of the spacer arm did not cause a significant alteration of the atomic charges, and very close

This journal is © The Royal Society of Chemistry 2011

Org. Biomol. Chem., 2011, **9**, 1443–1453 | 1447

Fig. 4 *Computed partial atomic charges of PY and haptens PYo5, PYa6 and PYs5.* Only those atoms showing a charge variation higher than 1% between PY and any of the haptens are depicted. Hydrogens are not included.

electronic similarities between PY and the immunizing haptens were found. In hapten PYs5, the hydrocarbon spacer chain is tethered to the benzene ring through a sulfur bridge that replaced the chlorine atom of PY. This substitution meant the highest observed modification of the electronic properties compared with the two other haptens (the partial charge at C1 in PYs5 changed by 37%). Nevertheless, this sort of replacement, which has been previously used for the design of haptens for chlorine-containing analytes,[16] is less drastic than if a C–C bond had been formed. In addition, the antibody with the highest affinity to PY was derived from hapten PYs5, so electronic charges did not account by themselves for the observed differences among immunizing haptens.

As a further step to understand the reason why hapten PYa6 was a poorer mimic of the PY molecule than haptens PYo5 and PYs5, the structure of the three synthesized haptens was modeled taking into account the flexibility of the spacer arm. In order to simplify this analysis, we assumed that in the synthetic haptens the common PY framework can adopt a conformational disposition similar to that of PY itself. A preliminary estimation of the preferred orientation of the spacer arm in each hapten was done by calculating the conformer with the lowest energy in aqueous solution when the two first C–C bonds of the spacer arm proximal to the backbone of the PY molecule were rotated independently

360° in 15° increments. From this study, we observed that the minimum energy conformers for haptens PYo5 and PYs5 showed a trend to display the linker away from the backbone of the molecule. On the contrary, the lowest energy conformers of PYa6 showed that the linker has a certain tendency to bend over the molecule (Fig. 5), a finding that provides a feasible explanation for the inferior performance of the PYa6 derivative as immunizing hapten.

Conclusions

In order to obtain antibodies endowed with appropriate binding properties to small organic molecules, optimal functionalized derivatives of the target analyte must be prepared. In the present study, multistep synthetic routes were carried out for a better understanding of the importance of the derivatization site. Molecular modeling studies indicated that, in the case of haptens PYo5 and PYs5, the spacer arm facilitated an adequate exposure of the skeleton of PY during the immune response. On the contrary, the central position of the linker in the molecule of PYa6 could have caused steric hindrance that impaired the formation of a deep and tight binding pocket, typical of most antibody–hapten interactions.[17] Therefore, interactions between the linker arm and the backbone of the molecule may occur not only if too long spacers are employed, as demonstrated in our previous paper,[5] but also because of an inappropriate tethering site. Acquisition of a larger body of knowledge and more profound studies are required in order to better understand the factors influencing the formation and stabilization of the antibody–analyte complex. In practice, these antisera—particularly those derived from haptens PYo5 and PYs5—should become very useful reagents for the preparation of immunoaffinity columns intended for PY purification and concentration, as well as for the development of immunochemical methods enabling the selective and sensitive determination of PY in incurred real samples.

Experimental

PY [methyl {2-[1-(4-chlorophenyl)pyrazol-3-yloxymethyl]-phenyl}methoxy carbamate] (CAS Registry No. 175013-18-0,
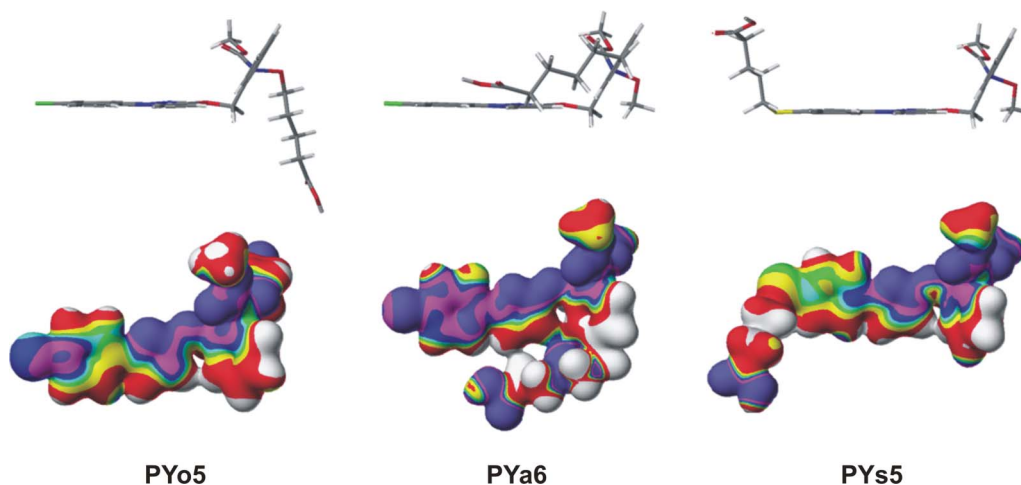
Fig. 5 *Most probable geometries and electron density surfaces colored by electrostatic potential from two different views of the three synthesized haptens.* Color codes are the same as in Fig. 3.

MW 387.8 g mol^{-1}) was purchased, Pestanal grade, from Riedel-de-Haën (Seelze, Germany). The methyl methoxy(o-tolyl)carbamate (1) used in this work was kindly provided by BASF AG (Limburgerhof, Germany). *tert*-Butyl hex-5-ynoate (8) and *tert*-butyl 5-bromopentanoate (15) were prepared from commercial hex-5-ynoic acid[18] and 5-bromopentanoic acid, respectively.[19] Methyl 2-(bromomethyl)phenyl(methoxy) carbamate (18) was prepared from tolylcarbamate 1.[20] All melting points were determined using a Kofler hot-stage apparatus or a Büchi melting point apparatus and are uncorrected. All NMR spectra were recorded in CDCl$_3$ or acetone-d_6 at rt on a Bruker AC-300 spectrometer (300.13 MHz for ^{1}H and 75.47 MHz for ^{13}C). The spectra were referenced to residual solvent protons in the ^{1}H NMR spectra (7.26 and 2.05 ppm) and to solvent carbons in the ^{13}C NMR spectra (77.0 and 30.83 ppm). Infrared spectra were measured as thin films between NaCl plates for liquid compounds and as KBr pellets for solids using a Nicolet Avatar 320 spectrometer. Electron-impact (EI) and fast atom bombardment (FAB) mass spectra (MS and HRMS) were obtained with a Micromass VG Autospec spectrometer. ELISA absorbances were read with a PowerWave HT microplate reader from BioTek Instruments (Winooski, VT, USA). A Voyager De-Pro workstation from Applied Biosystems was used for the analysis of the molecular weight of protein conjugates by matrix-assisted laser desorption ionization time-of-flight mass spectrometry (MALDI-TOF-MS).

Determination of minimum-energy conformations

The initial generation of low-energy conformations and geometry optimizations of PY was made using the conformational space search program CONFLEX6 from Conflex Corp. (Tokyo, Japan) running on Windows XP. The visualization and analysis interface BARISTA, a platform especially designed for conformational analyses, was used to create the initial parameters, and conformation search was carried out with MMFF94S (2006-11-24HGTEMP) parameters using the default configuration resources, except for the upper limit value of conformational search that was set to cover an area of 10 kcal mol^{-1} within the most stable conformation (SEL = 10).[21] The GBSA continuum solvation method was also introduced to evaluate the solvation energy contribution to the steric energy.[22] The energy distribution of conformers was established under steric energy analysis. Those conformations that were chemically significant (accounting for 99.8% of the computed population) were grouped based on dihedral angle values (refer to Table 1SI in the ESI†) and the lowest-energy conformation of each group was used to create a potential energy map in which the two dihedral angles differing within each group were rotated independently 360° in 10° increments using the PM3 semiempirical method, including the solvent effects of water as simulated by the COSMO solvation model. The potential energy conformation maps were constructed for each selected conformation with CAChe WorkSystem Pro from Fujitsu Ltd. (Tokyo, Japan) using the MOPAC_OpMap2_PM3_H$_2$O procedure. Several of the low-energy conformations obtained from each generated potential energy map were chosen and reoptimized, and the lowest-energy conformations thus obtained were selected as the minimum energy conformations of PY. Optimized geometries of haptens were also calculated using the semi-empirical

method PM3 with COSMO water simulation using dihedral angle increments of 15°. Electrostatic potential energy surfaces were mapped over electron density isosurfaces using the same force field. The electron density probability value used for all calculations was 0.01 electrons Å^{-3}.

Buffers and solutions

The following buffers were employed: PB, 100 mM sodium phosphate buffer, pH 7.4; PBS, 10 mM sodium phosphate buffer, pH 7.4 with 140 mM NaCl; PBST, PBS containing 0.05% (v/v) Tween 20; CB, 50 mM carbonate–bicarbonate buffer, pH 9.6; and washing solution, 150 mM NaCl containing 0.05% Tween 20. PY and all other analytes were prepared as concentrated solutions in *N*,*N*-dimethylformamide (DMF) and kept at −20 °C in amber glass vials.

Hapten synthesis

The synthesis of hapten PYo5 was previously published.[7] Hapten PYa6 was synthesized from methyl methoxy(o-tolyl)carbamate (1)[20] following the synthetic route detailed in Scheme 1 and hapten PYs5 was synthesized from commercial methyl (4-iodophenyl)hydrazine (12) following the procedure depicted in Scheme 2. Unless otherwise stated, organic extracts were successively washed with H$_2$O and brine, dried over anhydrous Na$_2$SO$_4$, and concentrated under vacuum. The characterization data of the synthetic intermediates can be found in the ESI.† All solvents were purified by distillation and, if required, they were dried according to standard methods.

Synthesis of PYa6

Methyl 4-iodo-2-methylphenyl(methoxy)carbamate (2). Ag$_2$SO$_4$ (1.097 g, 3.51 mmol) and I$_2$ (0.893 g, 3.52 mmol) were successively added to a solution of methyl methoxy(o-tolyl)carbamate (1) (680 mg, 3.48 mmol) in glacial acetic acid (9 mL), and the reaction mixture was stirred for 20 h at rt in the dark. After this time, a yellowish precipitate of AgI was formed, which was removed by filtration. The filtrate and washes were diluted with water and extracted with CH$_2$Cl$_2$. The combined organic extracts were successively washed with aqueous NaHCO$_3$, aqueous Na$_2$S$_2$O$_7$, brine, and dried. Evaporation of the solvent under vacuum gave 2 (1.093, 98%) as a viscous oil that had a purity greater than 95%, as judged by ^{1}H NMR analysis, and it was used in the next step without further purification.

Methyl 2-(bromomethyl)-4-iodophenyl(methoxy)carbamate (3). A solution of methoxycarbamate 2 (810 mg, 2.50 mmol) and bromine (3.21 g, 1.03 mL, 20.1 mmol, 8 equiv) in dry CCl$_4$ (90 mL) was irradiated with a mercury lamp (125 W) for 36 h at rt. The reaction mixture was washed with aqueous Na$_2$S$_2$O$_7$ and brine, and dried. The solvent was evaporated under vacuum to give an oily residue (885 mg) consisting in a mixture of monobrominated compound 3, the corresponding dibrominated derivative, and unreacted starting material that could not be separated by conventional chromatographic purification methods. The percent of 3 in the mixture was estimated to be 50–55% on the basis of the analysis of the mixture by NMR.

This journal is © The Royal Society of Chemistry 2011

Org. Biomol. Chem., 2011, **9**, 1443–1453 | 1449

1-(4-Chlorophenyl)-1H-pyrazol-3-ol (6). A solution of sodium ethoxide in ethanol, prepared by dissolving Na (882 mg, 38.3 mol) in anhydrous ethanol (27 mL), was added to a suspension of 4-chlorophenylhydrazine hydrochloride (**4**) (3.00 g, 16.75 mmol) in dry toluene (27 mL) stirred under nitrogen at 40 °C. After stirring at the same temperature for 10 min, methyl acrylate (7.21 g, 7.54 mL, 83.75 mmol) was added drop wise during 20 min and the resulting mixture was stirred for 1.5 h. The reaction mixture was concentrated in a rotary evaporator to remove most of the ethanol, then diluted with water (300 mL) and extracted with benzene. The benzene extracts were extracted with 5% sodium hydroxide and the combined aqueous basic phases were acidified with acetic acid to pH 6 and extracted with benzene. The organic layer was washed, dried, and concentrated to give nearly pure 1-(4-chlorophenyl)pyrazolidin-3-one (5) (2.35 g, 71%) as an amorphous solid.

The above solid (1.265 g, 6.43 mmol) and CuCl (68 mg, 0.32 mmol) were dissolved in DMF (13 mL) and O_2 was bubbled through the mixture during 3 h at rt. The reaction mixture was diluted with H_2O (100 mL) and then stirred for 1 h. The formed precipitate was filtered off, washed with water, and dried to afford a brownish solid that was crystallized from benzene to give **6** (993 mg, 80%) as a slightly colored solid; mp 190–192 °C (from benzene), at 174–176 °C flake-like crystals were transformed into needle like crystals (lit.,[10] mp 181–182 °C).

Methyl 2-((1-(4-chlorophenyl)-1H-pyrazol-3-yloxy) methyl)-4-iodophenyl(methoxy)carbamate (7). A mixture of pyrazolol **6** (186.3 mg, 0.96 mmol), benzyl bromide **3** (768 mg of the mixture obtained above from the bromination of methoxycarbamate **2**, containing approximately 1.0 mmol of **3**), and CsCO$_3$ (759 mg, 2.32 mmol) in anhydrous DMF (6 mL) was stirred at rt overnight. The reaction mixture was diluted with H_2O and extracted with ethyl acetate. The organic layer was washed and dried. Filtration and evaporation of the solvent was followed by column chromatography, using hexane–ethyl acetate 8 : 2 as eluent, to give **7** (395 mg, 80%) as an oil that solidified upon standing; mp 105–107 °C (from methanol).

***tert*-Butyl 6-(3-((1-(4-chlorophenyl)-1H-pyrazol-3-yloxy) methyl)-4-(methoxy(methoxycarbonyl)amino)phenyl)hex-5-ynoate (9).** Dry DMF (1.5 mL) and triethylamine (1.2 mL) were added to a mixture of aryl iodide **7** (241.5 mg, 0.468 mmol), *tert*-butyl hex-5-ynoate (**8**) (117.9 mg, 0.702 mmol), Cl$_2$Pd(PPh$_3$)$_2$ (9.3 mg, 0.13 µmol), and CuI (3.6 mg, 0.19 µmol) under nitrogen. The mixture was degassed through several freeze–thaw cycles, stirred at rt for 30 min and then at 60 °C for 4 h. The resulting brownish reaction mixture was cooled down, filtered through cotton and most of the triethylamine was removed under vacuum. The residue was diluted with ethyl acetate and washed, dried, and concentrated. Purification by silica gel chromatography, using hexane–ethyl acetate 9 : 1 as eluent, afforded compound **9** (255 mg, 98%) as an oil.

***tert*-Butyl 6-(3-((1-(4-chlorophenyl)-1H-pyrazol-3-yloxy) methyl)-4-(methoxy(methoxycarbonyl)amino)phenyl)hexanoate (10).** A solution of alkyne **9** (243 mg, 0.439 mmol) and Wilkinson's catalyst (12.2 mg, 0.013 mmol, 3%) in tetrahydrofuran (3 mL) was evacuated and purged under an atmosphere of hydrogen gas. Then, the hydrogen pressure was regulated to 4 atmospheres and the

reaction mixture was stirred at rt for 16 h. The solvent was removed under vacuum, and the residue was purified by chromatography, using hexane–ethyl acetate 9 : 1 as eluent, to furnish compound **10** (220 mg, 92%).

6-(3-((1-(4-Chlorophenyl)-1H-pyrazol-3-yloxy)methyl)-4-(methoxy(methoxycarbonyl)amino)phenyl)hexanoic acid (11, hapten PYa6). A solution of the *tert*-butyl ester **10** (203 mg, 0.364 mmol) in trifluoroacetic acid (1.5 mL) and CH_2Cl_2 (1.5 mL) was stirred at 0 °C until TLC [developed with hexane–ethyl acetate (7 : 3)] showed completion of the reaction (about 1 to 1.5 h). The reaction mixture was concentrated under vacuum without heating and the residue obtained was purified by silica gel chromatography, using 4% of methanol in CHCl$_3$ as eluent, to give the hapten PYa6 (**11**) (182 mg, 99%) as a slightly colored viscous oil; δ_H (CDCl$_3$) 7.70 (1H, d, J = 2.6 Hz, H-5 Pz), 7.55 (2H, m, part AA′ of the AA′BB′ system, J = 8.8, 2.5, 0.5 Hz, H-2, and H-6 ClPh), 7.47 (1H, d, J = 1.8 Hz, H-3 Ph), 7.37 (2H, m, part BB′ of the AA′BB′ system, J = 8.8, 2.5, 0.5 Hz, H-3, and H-5 ClPh), 7.27 (1H, d, J = 8.1 Hz, H-6 Ph), 7.18 (1H, dd, J = 8.1, 1.8 Hz, H-5 Ph), 5.94 (1H, d, J = 2.6 Hz, H-4 Pz), 5.30 (2H, s, OCH$_2$), 3.79 (3H, s, CO$_2$CH$_3$), 3.75 (3H, s, NOCH$_3$), 2.66 (2H, t, J = 7.7 Hz, H-6), 2.34 (2H, t, J = 7.4 Hz, H-2), 1.64 (4H, m, H-3 and H-5) and 1.40 (2H, m, H-4); δ_C (CDCl$_3$) 179.01 (C-1), 164.30 (C-3 Pz), 155.94 (NCO$_2$), 143.46 (C-1 Ph), 138.59 (C-1 ClPh), 134.92 and 134.40 (C-2 and C-4 Ph), 130.61 (C-4 ClPh), 129.34 (C-3 and C-5 ClPh), 128.87 and 128.58 (C-3 and C-5 Ph), 127.73 (C-5 Pz), 127.17 (C-6 Ph), 118.93 (C-2 and C-6 ClPh), 94.33 (C-4 Pz), 66.95 (OCH$_2$), 61.94 (NOCH$_3$), 53.52 (CO$_2$CH$_3$), 35.28 (C-6), 33.80 (C-2), 30.69 (C-5), 28.47 (C-4) and 24.43 (C-3); υ_{max}/cm^{-1} (NaCl) 3400–2800, 2933, 2861, 1735, 1707, 1546, 1501, 1481, 1358, 1094 and 751; *m/z* (EI) 441 (8%), 440 (6), 439 (22), 308 (9), 278 (10), 277 (18), 247 (16), 277 (17), 276 (10), 246 (100) and 194 (59); *m/z* (FAB) calcd for C$_{25}$H$_{29}$ClN$_3$O$_6$ (M$^+$ + H) 502.17449, found 502.17539; λ_{max} (PB)/nm 280 (ε/dm^3 mol^{-1} cm^{-1} 12.1) and 260 (11.7).

Synthesis of PYs5

1-(4-Iodophenyl)-1H-pyrazol-3-ol (14). A 1 M solution of potassium *tert*-butoxide in *tert*-butanol (1.2 mL, 1.2 mmol) was added to a solution of (4-iodophenyl)hydrazine (**12**) (234 mg, 1 mmol) in anhydrous toluene (1.2 mL) at rt under nitrogen. The mixture was warmed to 50 °C and then drop wise treated with *tert*-butyl acrylate (135 mg, 153 µL, 1.05 mmol). The reaction mixture was stirred at 50 °C for a few minutes, then cooled to rt, diluted with benzene, and extracted with 5% aqueous KOH. The aqueous layer was treated with excess CO_2 and the fuchsia solid formed was extracted with ethyl acetate (5 times). The combined organic layers were washed and dried. Filtration and evaporation of the solvent afforded a solid that was crystallized from benzene–acetone to give crystals of 1-(4-iodophenyl)pyrazolidin-3-one (**13**) (179 mg, 62%) as a brown solid; mp 142–143 °C (from benzene–acetone).

A mixture of the compound **13** obtained above (164 mg, 0.577 mmol) and CuCl (2.5 mg, 0.03 mmol) in DMF (2.5 mL) was stirred in the air until all the starting material was consumed (about 5 h). The reaction mixture was diluted with H_2O and the solid formed was collected by filtration, washed with cold water, and dried under vacuum to obtain pure 1-(4-iodophenyl)-1H-pyrazol-3-ol (**14**) (160 mg, 97%) as a cream color solid; needle-like

crystals from hexane–ethyl acetate began to sublimate at 190 °C and melted at 222–224 °C.

tert-Butyl 5-(4-(3-hydroxy-1H-pyrazol-1-yl)phenylthio)pentanoate (17). *tert*-Butyl 5-mercaptopentanoate (**16**) was prepared from *tert*-butyl 5-bromopentanoate (**15**) and thiourea with very high yield *via* formation of the thiouronium salt followed by cleavage with sodium pyrosulfite.[11] Then, a mixture of iodophenyl-pyrazolol **14** (200 mg, 0.70 mmol), thiol **16** (200 mg, 1.05 mmol), K_2CO_3 (193 mg, 1.40 mmol), CuI (7 mg, 0.035 mmol), and ethylene glycol (78 µL, 1.40 mmol) in 2-propanol (0.7 mL) was degassed through three freeze–pump–thaw cycles, sealed under vacuum, and heated at 80–85 °C with stirring for 24 h. The cooled reaction mixture was diluted with ethyl acetate and washed, dried, and concentrated. The brownish oily residue was purified by column chromatography, using hexane–ethyl acetate mixtures from 9 : 1 to 7 : 3 as eluent, to give, in order of elution, unreacted starting pyrazolol **14** (54 mg, 73% conversion) and compound 17 (130 mg, 70%) as a solid; mp 113–114 °C (from hexane–isopropanol).

tert-Butyl 5-(4-(3-(2-(methoxy(methoxycarbonyl)amino) benzyloxy)-1H-pyrazol-1-yl)phenylthio)pentanoate (19). A mixture of compound **17** (99 mg, 0.284 mmol), methyl 2-(bromomethyl)-phenyl(methoxy)carbamate (**18**, prepared by benzylic bromination of tolylcarbamate **1** with *N*-bromosuccinimide and azaisobutyronitrile in CCl_4 at reflux)[8] (117 mg, 0.427 mmol), and $CsCO_3$ (139 mg, 0.427 mmol) in anhydrous DMF (1.2 mL) was stirred at rt overnight under nitrogen. The reaction mixture was diluted with ethyl acetate and washed, dried, filtered, and then evaporated to dryness. Purification by column chromatography, using hexane–ethyl acetate 9 : 1 as eluent, afforded compound **19** (134 mg, 89%) as a viscous oil.

5-(4-(3-(2-(Methoxy(methoxycarbonyl)amino)benzyloxy)-1H-pyrazol-1-yl)phenylthio)pentanoic acid (20, hapten PYs5). A solution of the *tert*-butyl ester **19** (107 mg, 0.197 mmol) in a 1 : 1 mixture of trifluoroacetic acid and CH_2Cl_2 (4 mL) was stirred at 0 °C for 1 h. Work-up of the reaction mixture as described above for the hydrolysis of **10** to **11**, followed by chromatography on silica gel and using $CHCl_3$–methanol 95 : 5 as eluent, afforded hapten PYs5 (**20**) (86 mg, 90%) as a colorless viscous oil; δ_H ($CDCl_3$) 7.69 (1H, d, *J* = 2.6 Hz, H-5 Pz), 7.66 (1H, m, H-4 Ph), 7.51 (2H, m, part AA′ of the AA′BB′ system, *J* = 8.8, 2.5, 0.5 Hz, H-2 and H-6 SPh), 7.40–7.35 (3H, m, H-3, H-5 and H-6 Ph overlapped with the part BB′ of the AA′BB′ system corresponding to H-3 and H-5 SPh), 5.90 (1H, d, *J* = 2.6 Hz, H-4 Pz), 5.34 (2H, s, OCH_2), 3.79 (3H, s, CO_2CH_3), 3.75 (3H, s, $NOCH_3$), 2.91 (2H, t, *J* = 7.1 Hz, H-5), 2.36 (2H, t, *J* = 7.0 Hz, H-2) and 1.72 (4H, m, H-3 and H-4); δ_C ($CDCl_3$) 178.86 (C-1), 164.10 (C-3 Pz), 155.84 (NCO_2), 138.48 and 137.30 (C-1 and C-2 Ph), 134.77 (C-1 SPh), 132.69 (C-4 SPh), 130.95 (C-3 and C-5 SPh), 128.85, 128.80 and 128.48 (C-3, C-4 and C-5 Ph), 127.66 (C-5 Pz), 127.01 (C-6 Ph), 118.29 (C-2 and C-6 SPh), 94.05 (C-4 Pz), 66.79 (OCH_2), 62.09 ($NOCH_3$), 53.54 (CO_2CH_3), 33.99 (C-5), 33.35 (C-2), 28.33 (C-4) and 23.58 (C-3); υ_{max}/cm^{-1} (NaCl) 3500–2800, 3142, 3044, 2954, 1793, 1708, 1545, 1480, 1358, 1267, 1100 and 737; *m/z* (EI) 485 (M⁺, 0.1%), 467 (1), 454 (1.5), 453 (4), 437 (6), 425 (7), 424 (18), 423 (76), 422 (4), 379 (3), 291 (30), 162 (12) and 132 (100); *m/z* (EI) calcd

for $C_{24}H_{27}N_3O_6S$ 485.16206, found 485.16249; λ_{max} (PB)/nm 280 (ε/dm^3 mol^{-1} cm^{-1} 19.2) and 260 (8.15).

Protein conjugate preparation

All of the synthesized haptens contained a free carboxylic group for protein conjugation. The hapten-to-protein MR of each bioconjugate was calculated by MALDI-TOF-MS and by differential absorbance measurements. For MALDI-TOF-MS analysis, a fraction of each conjugate solution was extensively dialyzed against pure water at 4 °C and lyophilized. Samples were resuspended in acetonitrile–water 7 : 3 containing 0.1% trifluoroacetic acid, and they were charged into the plate in between two layers of sinapinic acid.

Immunizing conjugates

BSA conjugates were prepared by the active ester procedure. Briefly, 20 µmol of hapten in DMF was mixed with 20 µmol of *N*-hydroxysuccinimide and 20 µmol of *N,N*-dicyclohexylcarbodiimide also in DMF. Additional DMF was added to bring the final concentration of all reagents to 50 mM. Hapten activation was left to occur overnight at rt in amber vials. The day after, the reaction was centrifuged and the supernatant was collected. Next, 200 µL of activated hapten solution was added drop wise to 1.0 mL of a 15.0 mg mL⁻¹ BSA solution in CB. The coupling reaction was allowed to happen during 4 h at rt with moderate stirring. The initial hapten-to-protein MR in the reaction mixture was approximately 44 : 1. Finally, the conjugate was separated from uncoupled hapten by gel filtration on Sephadex G-25, using PB as eluent. The purified bioconjugate was diluted to 1.0 mg mL⁻¹ with PB and stored at −20 °C. For differential absorbance measurements, the absorbance values of the conjugate at 280 and 260 nm were considered.

Coating conjugates

In this case, the coupling reaction of the hapten to the carrier protein was accomplished by the mixed anhydride procedure. Basically, 18 µmol of hapten was dissolved in 180 µL of DMF and mixed with 18 µmol of tributylamine and 18 µmol of isobutyl chloroformate also in DMF. The concentration of all reagents was brought to 90 mM with DMF and the hapten was left to be activated during 1 h at rt. Next, 100 µL of activated hapten solution was added drop wise to 2.0 mL of a 15.0 mg mL⁻¹ OVA solution in CB. The coupling reaction was carried out during 2.5 h at rt with moderate stirring. The initial hapten-to-protein MR in the reaction mixture was approximately 13 : 1. Conjugates were processed and stored as described above.

Tracer conjugates

The mixed anhydride method was also used to prepare the corresponding enzyme conjugates. First, haptens were activated as described above and a 1/10 dilution in DMF was prepared after the incubation step. Next, 100 µL of this dilution was added drop wise to a 1.0 mL solution of HRP at 2.2 mg mL⁻¹ in CB. The coupling reaction was incubated for 4 h at rt with moderate stirring. The initial hapten-to-protein MR in the reaction mixture was approximately 18 : 1. The tracer was

This journal is © The Royal Society of Chemistry 2011

Org. Biomol. Chem., 2011, **9**, 1443–1453 | 1451

separated from uncoupled hapten by gel filtration on Sephadex G-25. For differential absorbance measurements, the absorbance values of the conjugate at 400 and 280 nm were considered in this case. The purified tracer was brought to 1.0 mg mL^{-1} with PB and diluted 1/2 with PBS containing 1% (w/v) BSA and 0.01% (w/v) thimerosal. The conjugate was stored at -20 °C in amber glass vials for long-term preservation and a working aliquot was kept at 4 °C.

Antiserum production

Animal manipulation was performed in compliance with the laws and guidelines of the Spanish Ministry of Science and Innovation (RD 1201/2005 and law 32/2007) and according to the European Directive 2003/65/EC (amending general Council Directive 86/609/EEC) concerning the protection of animals used for experimental and other scientific purposes. Two New Zealand white female rabbits weighing 1–2 kg were immunized by subcutaneous injection with 0.3 mg of conjugate BSA–PYo5, BSA–PYa6, or BSA–PYs5 following described procedures.[23] For further details see the ESI.†

Competitive immunoassays

All antisera were evaluated in the two classical cELISA formats using both homologous and heterologous conjugates. Eight-channel electronic pipettes were employed for rapid and precise liquid dispensing. Microplates were washed four times with washing solution using a 96-channel ELx405 washer from BioTek Instruments (Winooski, VT, USA). After the assay, the absorbance was read at 492 nm with a reference wavelength at 650 nm. Sigmoidal curves were mathematically fitted to a four-parameter logistic equation using the SigmaPlot software package from SPSS Inc. (Chicago, IL, USA). The antiserum titer was defined as the reciprocal of the dilution that results in a maximum absorbance value (A_{max}) around 1.0 reached at the zero dose of analyte when assayed using the indirect competitive format with the homologous conjugate at 1.0 µg mL^{-1}. Antibody affinity was estimated as the concentration of analyte that reduced 50% (IC_{50}) the A_{max} value, and the assay limit of detection was defined as the IC_{10} of the inhibition curve.

Conjugate-coated indirect assays

ELISA plates were coated with 100 µL per well of OVA conjugate solution at 1.0 and 0.1 µg mL^{-1} in CB by overnight incubation at rt. Serial three-fold antisera dilutions (from 1/1500 to 1/5 × 10^5) were prepared in PBST. Each plate column received a complete standard curve of the analyte in PBS (50 µL per well) followed by a given antiserum dilution (50 µL per well). The same distribution of the reagents was repeated for each plate with a different conjugate. The immunological reaction took place during 1 h at rt, and plates were washed again as described. Next, 100 µL per well of a 1/10000 dilution of goat anti-rabbit IgG peroxidase conjugate in PBST was added, and plates were incubated 1 h at rt. After washing four times, the retained peroxidase activity was determined by addition of 100 µL per well of freshly prepared 2.0 mg mL^{-1} of OPD and 0.012% (v/v) H_2O_2 in 25 mM citrate and 62 mM sodium phosphate buffer, pH 5.4. The enzymatic reaction was stopped after 10 min with 100 µL of 2.5 M H_2SO_4.

Antibody-coated direct assays

Microplates were coated with 100 µL per well of a 1/3000, 1/10000, and 1/30000 dilution of a given antiserum in CB by overnight incubation at rt. After four washes, 50 µL per well of PY standard curve was dispensed to each plate column and immediately 50 µL per well of a different concentration of a given enzyme tracer was added. In this case, serial three-fold dilutions in PBST of the HRP conjugate (from 600 to 2 ng mL^{-1}) were prepared. The same array of reagent concentrations was distributed in another plate that had previously been coated with a different antiserum. The immunological reaction was carried out during 1 h at rt and the enzyme activity was revealed as described before.

Notes and references

1 K. Landsteiner, *Koninkl. Akad. Wet. Amst. Verslag*, 1921, **30**, 329.
2 For example, (a) S. Lu, Y. Zhang, J. Liu, C. Zhao, W. Liu and R. Xi, *J. Agric. Food Chem.*, 2006, **54**, 6995; (b) J. V. Mercader, C. Suárez-Pantaleón, C. Agulló, A. Abad-Somovilla and A. Abad-Fuentes, *J. Agric. Food Chem.*, 2008, **56**, 2581.
3 (a) Y. J. Kim, Y. A. Cho, H. S. Lee, Y. T. Lee, S. J. Gee and B. D. Hammock, *Anal. Chim. Acta*, 2003, **475**, 85; (b) Y. H. Liu, M. J. Jin, W. J. Gui, J. L. Cheng, Y. R. Guo and G. N. Zhu, *Anal. Chim. Acta*, 2007, **591**, 173.
4 (a) Z. Wang, Y. Zhu, S. Ding, F. He, R. C. Beier, J. Li, H. Jiang, C. Feng, Y. Wan, S. Zhang, Z. Kai, X. Yang and J. Shen, *Anal. Chem.*, 2007, **79**, 4471Review; (b) Z. L. Xu, Y. D. Shen, R. C. Beier, J. Y. Yang, H. T. Lei, H. Wang and Y. M. Sun, *Anal. Chim. Acta*, 2009, **647**, 125.
5 (a) D. W. Barlett, J. M. Clough, C. R. A. Godfrey, J. R. Godwin, A. A. Hall, S. P. Heaney and S. J. Maund, *Pestic. Outlook*, 2001, **12**, 143; (b) H. Sauter, in *Modern Crop Protection Compounds*, ed. W. Kraemer and U. Schirmer, Willey-VCH, Weinheim, Germany, 2007, pp. 457-495.
6 For example, (a) B. Ballesteros, D. Barceló, F. Sánchez-Baeza, F. Camps and M. P. Marco, *Anal. Chem.*, 1998, **70**, 4004; (b) R. Galve, F. Camps, F. Sánchez-Baeza and M. P. Marco, *Anal. Chem.*, 2000, **72**, 2237; (c) W. L. Shelver, Y. S. Keum, H. J. Kim, D. Rutherford, H. H. Hakk, A. Bergman and Q. X. Li, *J. Agric. Food Chem.*, 2005, **53**, 3840.
7 J. V. Mercader, C. Suárez-Pantaleón, C. Agulló, A. Abad-Somovilla and A. Abad-Fuentes, *J. Agric. Food Chem.*, 2008, **56**, 7682.
8 M. Ohnishi, S. Tajima, Y. Yamamoto and H. Kanno, *Eur. Pat.*, 619301 A2, 1994.
9 A. Liu, X. Wang, X. Ou, M. Huang, C. Chen, S. Liu, L. Huang, X. Liu, C. Zhang, Y. Zheng, Y. Ren, L. He and J. Yao, *J. Agric. Food Chem.*, 2008, **5**, 6562.
10 H. König, N. Götz, U. Klein and K. Eller, *US Pat.*, 5922886 A1, 1999.
11 A. Polina, K. Kalina, H. Karsten and T. Dimiter, *Cent. Eur. J. Chem.*, 2005, **3**, 658.
12 (a) M. Adamczyk, A. Buko, Y. Y. Chen, J. R. Fishpaugh, J. C. Gebler and D. D. Johnson, *Bioconjugate Chem.*, 1994, **5**, 631; (b) K. V. Singh, J. Kaur, G. C. Varshney, M. Raje and C. R. Suri, *Bioconjugate Chem.*, 2004, **15**, 168.

1452 | *Org. Biomol. Chem.*, 2011, **9**, 1443–1453

This journal is © The Royal Society of Chemistry 2011

13 R. C. Boro, K. V. Singh and C. R. Suri, *J. AOAC Int.*, 2009, **92**, 1773.

14 C. S. Ra and G. Park, *Bull. Korean Chem. Soc.*, 2002, **23**, 1199.

15 N. Sanvicens, F. Sánchez-Baeza and M. P. Marco, *J. Agric. Food Chem.*, 2003, **51**, 3924.

16 (*a*) R. Matsuo, K. Nishi, K. Morimune, H. Okawa and S. Miyake, *Jap. Pat.*, 2005035893, 2005; (*b*) J. J. Manclús, J. Primo and A. Montoya, *J. Agric. Food Chem.*, 1996, **44**, 4052.

17 M. Lee, P. Lloyd, X. Zhang, J. M. Schallhorn, K. Sugimoto, A. G. Leach, G. Sapiro and K. N. Houk, *J. Org. Chem.*, 2006, **71**, 5082.

18 G. Bartoli, M. Bosco, A. Carlone, R. Dalpozzo, E. Marcantoni, P. Melchiorre and L. Sambri, *Synthesis*, 2007, 3489.

19 S. Connolly, C. Bennion, S. Botterell, P. J. Croshaw, C. Hallam, K. Hardy, P. Hartopp, C. G. Jackson, S. J. King, L. Lawrence, A. Mete, D. Murray, D. H. Robinson, G. M. Smith, L. Stein, I. Walters, E. Wells and W. J. Withnall, *J. Med. Chem.*, 2002, **45**, 1348.

20 B. Mueller, H. Sauter, F. Roehl, R. Doetzer, G. Lorenz and E. Ammermann, *Pat.*, WO 9315046 A1, 1993.

21 (*a*) H. Goto and E. Osawa, *J. Am. Chem. Soc.*, 1989, **111**, 8950; (*b*) H. Goto and E. Osawa, *J. Chem. Soc., Perkin Trans. 2*, 1993, 187.

22 D. Qiu, P. S. Shenkin, F. P. Hollinger and W. C. Still, *J. Phys. Chem. A*, 1997, **101**, 3005.

23 C. Suárez-Pantaleón, J. V. Mercader, C. Agulló, A. Abad-Somovilla and A. Abad-Fuentes, *J. Agric. Food Chem.*, 2010, **58**, 8502.

This journal is © The Royal Society of Chemistry 2011

Org. Biomol. Chem., 2011, **9**, 1443–1453 | 1453